MONTHLY WEATHER REVIEW

SOME ASPECTS OF A CYCLE OF AVAILABLE POTENTIAL ENERGY [1]

JAY S. WINSTON AND ARTHUR F. KRUEGER

Meteorological Satellite Laboratory, U.S. Weather Bureau, Washington, D.C.

[Manuscript received April 27, 1961]

ABSTRACT

A large-scale cycle of available potential energy in the Northern Hemisphere over a period of about two weeks during late December 1958 and early January 1959 has been investigated in some detail. During this cycle the zonal available potential energy first built up strongly to a maximum, and then when it began to decline, increases in eddy available and eddy kinetic energy took place. These changes in the energy parameters were well related to variations in the poleward heat transport, large values of which signify substantial conversions from zonal to eddy available potential energy, and to variations in the conversion between potential and kinetic energy. Furthermore some estimates of the generation of available potential energy show good consistency with the available potential energy variations. Examination of this cycle of available potential energy on a regional basis indicates that it was almost completely dominated by developments over North America and vicinity. The synoptic events associated with this energy cycle are also illustrated.

1. INTRODUCTION

Satellite observations of solar and terrestrial radiation will soon be available in sufficient quantity to provide the first direct measurements of the global heat budget. As radiation is measured on a continuing day-by-day basis it will be of great interest to study not only the large-scale spatial and temporal variations in this basic planetary heating, but also the manner in which the atmosphere reacts to it. Since this heating is indeed basic in nature, any clear-cut reactions of the atmosphere to it would most likely be found in some of the more fundamental atmospheric parameters that directly measure the large-scale energetics of the circulation. In particular it seems appropriate to investigate the role of radiational heating with respect to the zonal and eddy components of kinetic and available potential energy as defined, for example, by Lorenz [4].

These various energy components and the typical flow

of energy from and to the environment and between various forms are illustrated schematically in figure 1 in the manner presented by Lorenz [3]. Here it is seen that diabatic heating of the atmosphere (actually differential heating between high and low latitudes) builds up the zonal available potential energy, which is basically a function of the latitudinal variance in temperature, or essentially a measure of the strength of latitudinal thermal gradients. As the zonal available energy keeps increasing, the strengthening thermal gradients lead to baroclinic instability and the growth of eddies. Thus eddy available potential energy (increasing thermal differences within latitude circles) increases at the expense of the zonal available energy as northward heat transport increases to relieve the excessive thermal gradients. Some of this increased eddy potential energy is then converted to eddy kinetic energy by means of direct thermal circulations (upward motion in the warm air, downward motion in the cold air) occurring in the eddies, or major cyclone waves. Differential heating relative to these eddies along
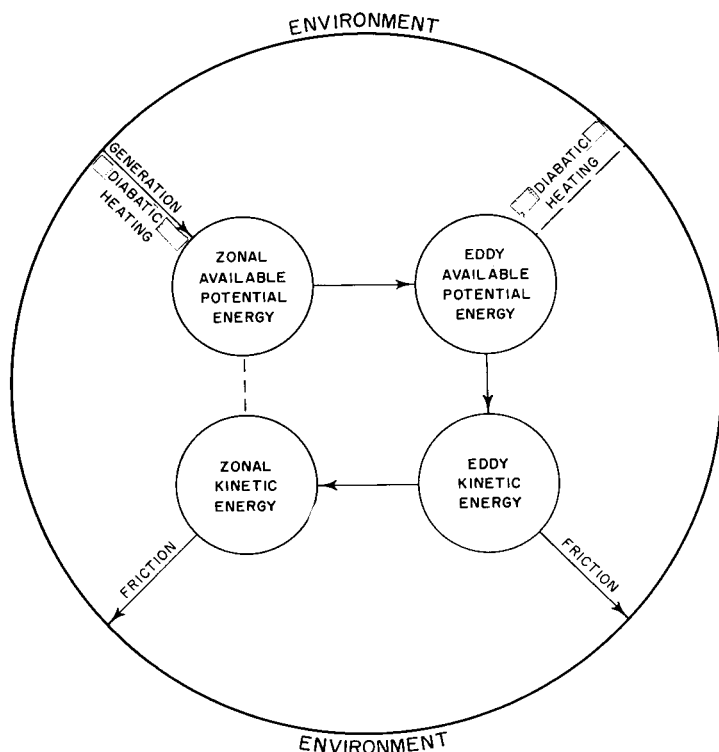
FIGURE 1.—Proposed energy cycle for the earth's atmosphere (after Lorenz [3]). Arrows indicate prevailing directions of energy transformations. Dashed lines indicate that there is apparently no prevailing direction.

latitude circles may either generate or dissipate the eddy available energy—a predominant trend in one direction or the other has not as yet been definitely established. Eddy kinetic energy is partially dissipated by friction and partially converted to zonal kinetic energy (much of the conversion being associated with the poleward transfer of momentum). The zonal kinetic energy is mainly subject to dissipation by friction, but a portion of it may be converted back into zonal available potential energy.

This typical energy flow picture has been generally substantiated by empirical evaluations of energy conversion terms (White and Saltzman [13]; Wiin-Nielsen [14]; Saltzman and Fleisher [10]; Jensen [1]). Although this mode of energy flux is representative of conditions that apparently must prevail on the average, it is realized that the generation and transformation of atmospheric energy may very well vary in both amount and direction at various times. This is the case both in the seasonal sense and also over time periods as short as a week or even a day, particularly when the energy in only one hemisphere or less is considered.

To investigate more closely the behavior of the energy cycle over various time and geographic scales a program for regular daily computation of several atmospheric energy parameters of the Northern Hemisphere has been initiated (Winston [16]). As a substantial sample of such calculations accumulate, it will be possible to document the energy cycle more precisely. Moreover, as radiation data

observed by satellites also accumulate, there will be an opportunity to calculate the generation of available potential energy (primarily the zonal component) and to study the reactions of the energy cycle to variations in this radiant energy. These are areas of study for the future, however.

For the present it is of interest to illustrate an actual case of a pronounced cycle of available potential energy which occurred during a pilot period of 42 days of energy computations in the winter of 1958–1959 (Winston [16]). This case seemed to fit the idealized energy flow picture to such a marked degree that it was of interest to examine it in some detail. Presentation of this case is of special significance because it is, to our knowledge, the first time that a cycle of large-scale available potential energy has been investigated for the actual atmosphere. In general circulation model experiments, on the other hand (Phillips [8]; Smagorinsky [12]), there has been extensive "day-by-day" calculation of potential and kinetic energy and energy transformations. Yet it is surprising that there has not been a like body of data computed from the real atmosphere to check similarities of the models and the observed time variations of the atmospheric energetics. Occasionally the energy cycle in the models has been compared to the index cycle of the atmosphere, which was described in detail by Rossby and Willett [9], and indeed the energy cycle and index cycle in a gross sense are often similar phenomena. However, as some experience has been gained with energy parameters, it has been found that the index cycle and the energy cycle do not always occur at the same time and with the same degree of intensity. To a great extent this is due to physically real differences in the behavior of the zonal winds as contrasted with the energetics of the flow. But also it is in part due to the inadequacy of the zonal index as a general circulation parameter. In fact, if one stresses the broader connotation that the term "index cycle" has attained, particularly in terms of cold air penetrations to lower latitudes and expanded circumpolar westerlies (Namias [5]; Rossby and Willett [9]), then it is highly probable that the dynamic and thermodynamic consequences of the energy cycle are truly more descriptive of these typical "index-cycle" phenomena than any index variations themselves. Thus, the expedient of verifying energetics of general circulation models in the real atmosphere by means of the index cycle is a patently crude procedure. It must be pointed out, however, that there have been comparisons of the *average* energetics of models with *average* values of energy transformations computed for the atmosphere.

The first published calculations of available potential energy for the Northern Hemisphere in the actual atmosphere, which were made at about the same time as those calculated by us, are some average values for the month of February 1959 (Saltzman and Fleisher [10]). Their results consist not only of monthly average values of total, zonal, and eddy available potential energy, but also the components of the eddy available energy for individual

wave numbers around latitude circles. It is believed that the present study of one particular energy cycle provides some interesting material which is complementary to that of Saltzman and Fleisher and which also aids in the physical comprehension of the atmospheric energy cycle.

2. DEFINITIONS AND METHODS OF COMPUTATION

The average available potential energy per unit area over the entire earth's atmosphere may be expressed by the following approximate equation, as derived by Lorenz [4]:

$$\overline{A} = \frac{1}{2} \int_0^{\overline{p}_0} (\Gamma_d - \overline{\Gamma})^{-1} \overline{T}^{-1} \overline{(T')^2} dp, \tag{1}$$

where bars within the integral refer to averages over an entire isobaric surface, T is temperature, Γ_d is the dry adiabatic lapse rate, $\overline{\Gamma}$ is the lapse rate, T' is the deviation of the temperature at any given point on the isobaric surface from its average value in that surface, p is pressure, and $\overline{p}_0$ is the average pressure at the surface of the earth. It should be noted that over short time periods (i.e., of the order of days, weeks, or perhaps a month) variations of available potential energy are essentially dependent upon variations in the spatial variance of temperature on isobaric surfaces, $\overline{(T')^2}$, since the mean temperature and mean lapse rates within an isobaric surface are relatively constant with time. In a longer-period sense (e.g., over several months) the time variations in available potential energy are, however, also influenced to a moderate degree by changes in mean lapse rate and to a lesser extent by changes in mean temperature.

Available potential energy may also be expressed in terms of two components, a zonal and an eddy component (Lorenz [4]). The expression for zonal available potential energy is

$$\overline{A}_Z = \frac{1}{2} \int_0^{\overline{p}_0} (\Gamma_d - \overline{\Gamma})^{-1} \overline{T}^{-1} \overline{[T]'^2} dp, \tag{2}$$

where the bracket refers to a latitudinal average and $[T]'$ is the departure of the latitudinal average temperature from the overall mean temperature. The expression for eddy available potential energy is

$$\overline{A}_E = \frac{1}{2} \int_0^{\overline{p}_0} (\Gamma_d - \overline{\Gamma})^{-1} \overline{T}^{-1} \overline{(T^*)^2} dp, \tag{3}$$

where T^* is the departure of the temperature at any point from its latitudinal average value. Thus, zonal available potential energy is mainly dependent upon the variance of the average latitudinal temperatures, or essentially upon the strength of the north-south thermal gradients, while eddy available potential energy is mainly a function of the variance of temperature within latitude circles, having a minimum value when isotherms are parallel to the latitude circles and having maximum

values when the isotherms display a wave pattern of large amplitude.

In attempting to calculate available potential energy in the actual atmosphere from synoptic data it is necessary to restrict the computations to a limited area where analyzed temperature data are available. In the calculations presented here, the area considered was the Northern Hemisphere from latitude 30° northward. Temperatures [2] at 700 mb. were used to represent the temperature field in the entire troposphere, and the calculations, which were made by means of a desk computer, were considered to apply to the layer between 1000 and 250 mb. No attempt has been made to weight these energy calculations for pressures less than 250 mb., since the available potential energy would tend to be much smaller in most of the more stable stratospheric layers than in tropospheric layers of comparable pressure intervals. A few tests comparing available potential energy computed from data throughout the troposphere and stratosphere, with values using 700-mb. temperatures only, show that the use of 700-mb. temperatures alone provides a good approximation to the available potential energy through the depth of the atmosphere. Another approximation in these calculations is the use of the standard atmosphere lapse rate for $\overline{\Gamma}$.

The average kinetic energy per unit area over the entire atmosphere may be expressed as follows (cf., Lorenz [4]):

$$\overline{K} = \frac{1}{2} g^{-1} \int_0^{\overline{p}_0} \overline{V^2} dp, \tag{4}$$

where g is the acceleration of gravity, V is the horizontal wind speed, and the bar within the integral again represents averaging over an entire isobaric surface. Kinetic energy may also be expressed in two components, zonal kinetic energy and eddy kinetic energy, the expressions for which are respectively as follows:

$$\overline{K}_Z = \frac{1}{2} g^{-1} \int_0^{\overline{p}_0} \overline{[V]^2} dp, \tag{5}$$

and

$$\overline{K}_E = \frac{1}{2} g^{-1} \int_0^{\overline{p}_0} \overline{(V^*)^2} dp, \tag{6}$$

where $[V]$ is the average wind for each latitude circle and V^* is the deviation of the wind from its latitudinal average value. Kinetic energy and its components were computed by means of a machine program which had previously been devised by C. L. Bristor. This program makes use of 500-mb. geostrophic winds obtained from 500-mb. height data of the Joint Numerical Weather Prediction (JNWP) Unit on their octagonal grid, which fully covers the area between about latitude 20° N. and the pole.

Expressions for time rates of changes of available potential and kinetic energy are also pertinent. Following Lorenz [4] we may write the following expressions for the local changes of energy:

---

[2] Temperature data recorded at 5° latitude and 10° longitude intervals (diamond grid) by the Extended Forecast Section of the Weather Bureau were used.

$$\frac{\partial \bar{A}}{\partial t}=-C+G \tag{7}$$

and

$$\frac{\partial \bar{K}}{\partial t}=C-D, \tag{8}$$

where

$$C=-Rg^{-1}\int_0^{\bar{p_0}} p^{-1}\overline{T\omega}\,dp, \tag{9}$$

$$G=g^{-1}\int_0^{\bar{p_0}} \Gamma_d(\Gamma_d-\overline{\Gamma})^{-1}\overline{T}^{-1}\overline{T'Q'}dp, \tag{10}$$

and

$$D=-g^{-1}\int_0^{\bar{p_0}} \overline{\mathbf{V}\cdot\mathbf{F}}dp. \tag{11}$$

In these expressions C represents the conversion between potential and kinetic energy, G is the generation of available potential energy, D is the frictional dissipation of kinetic energy, R is the gas constant for dry air, ω is equal to dp/dt (vertical motion in pressure coordinates), Q is the rate of addition of heat per unit mass, and $\mathbf{F}$ is the frictional force.

Generation of available potential energy is greatest when there is a high positive covariance between heating and temperature (equation (10)). In other words, when the atmosphere is heated where the temperature is high and cooled where the temperature is low there is considerable generation of available potential energy. The energy conversion term appears with opposite sign in equations (7) and (8). Energy is converted from available potential energy to kinetic energy when there is a correlation between vertical motion and temperature such that upward motion occurs in the warm air and downward motion occurs in the cold air (equation (9)). On the other hand, when the vertical motion field is reversed relative to the temperature field, i.e., downward motion in the warm air and upward motion in the cold air, the kinetic energy is converted to available potential energy.

It is obvious from these expressions that the place where radiational heating plays an important role is in the generation of available potential energy (equation (10)). This will be one of the most important terms to evaluate when satellite radiation data become available, and of course, it will be important to compare these evaluations of the generation term with the observed variations in available potential energy. At present, however, some calculations of the energy generation term can be made from indirect estimates of heating on a hemispheric scale (Wiin-Nielsen and Brown [15]).

The conversion term (equation (9)) is also of considerable interest in understanding the time variations of both kinetic and available potential energy. From data kindly provided by A. Wiin-Nielsen, some evaluations of this term have been made. These data are based on initial vertical motions and thicknesses available as a by-product of the operational baroclinic numerical prediction calculations of the JNWP Unit. These data were used by both Wiin-Nielsen [14] and Saltzman and Fleisher [10] to obtain calculations of this energy conversion term.

Expressions for conversion and generation of zonal and eddy components of available potential and kinetic energy are also given by Lorenz [4], but it is beyond the scope of this paper to present all of them here. It is pertinent, however, to write the expression for the conversion between zonal and eddy available potential energy, C_A, which is as follows:

$$C_A=-\frac{R}{g}\int_0^{\bar{p_0}} \frac{\bar{\theta}}{\overline{T}}\overline{\left([T^*v^*]\frac{\partial}{\partial y}+[T^*\omega^*]'\frac{\partial}{\partial p}\right)\left(\frac{\Gamma_d}{\Gamma_d-\overline{\Gamma}}\frac{[T]'}{\theta}\right)}dp, \tag{12}$$

where θ is potential temperature, $*$ denotes a deviation from a latitudinal average value, and $[\ ]'$ denotes a deviation of a latitudinal average value from the mean value over the entire isobaric surface. It will be noted that basically this conversion involves the products of the horizontal transport of sensible heat and the north-south temperature gradient and of the vertical transport of heat and the vertical temperature gradient.

In the discussion that follows only the northward heat transport itself is calculated. This transport, H, across a given latitude circle, ϕ_0, in a layer between two constant pressure surfaces, p_1 and p_2, is obtained through the following approximate expression:

$$H=\frac{c_p a \cos\phi_0(p_2-p_1)\Delta\lambda}{g}\sum v^*T^*, \tag{13}$$

where a is the radius of the earth, c_p is the specific heat at constant pressure, v is the meridional wind component, and λ is longitude. In the evaluation of (13), p_2 is taken as 850 mb. and p_1 as 500 mb., v^* and T^* are average values in the layer 850–500 mb., and the summation is over 72 intervals of $\Delta\lambda$, or 5° of longitude, around the latitude circle. Further treatment of the assumptions used in this calculation, including the use of geostrophic flow, has already been given elsewhere (Winston [16]).

3. DESCRIPTION OF THE ENERGY CYCLE AND VARIATIONS IN PARAMETERS ASSOCIATED WITH ENERGY CONVERSIONS

The day-to-day variations of the available potential energy, and its zonal and eddy components for the period of interest are shown in figure 2. It may be seen that the major cycle of buildup and breakdown in the total available potential energy between December 24 and January 7 mainly reflected the variation in the zonal component of the available potential energy. This is essentially indicative of the buildup of strong thermal gradients between latitude circles up to a peak on January 1, which was then followed by a very substantial breakdown in these thermal gradients between January 1 and 10. The eddy available potential energy remained at a nearly
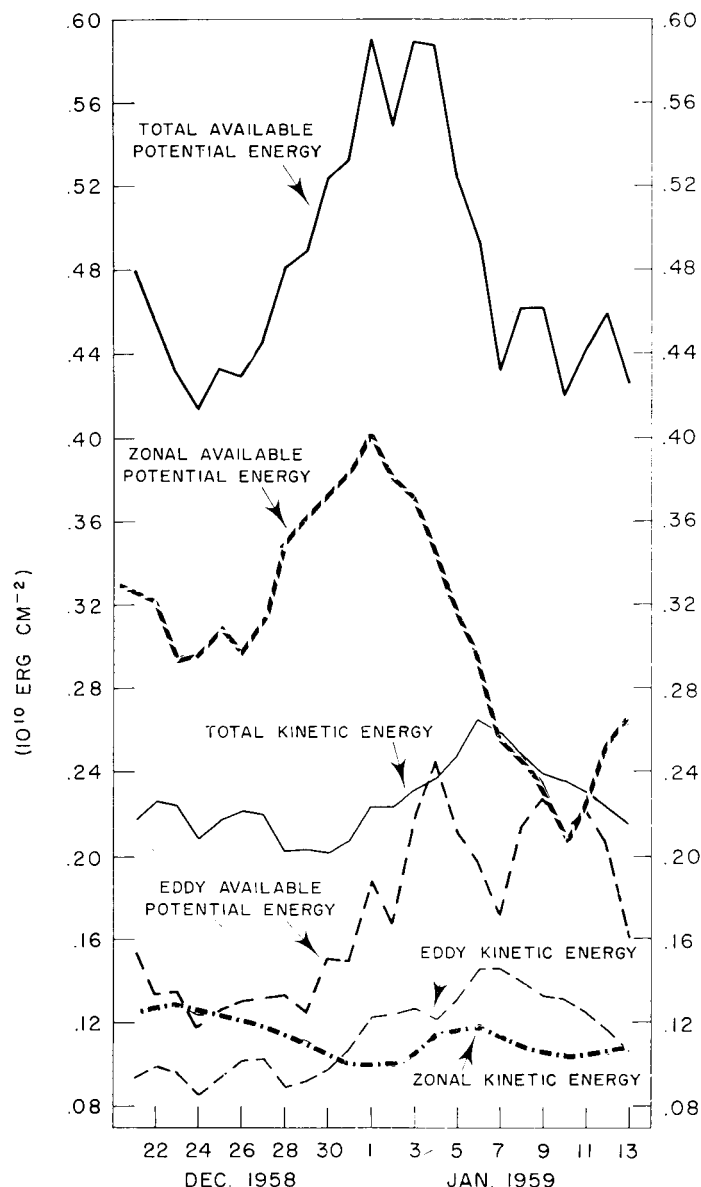
FIGURE 2.—Available potential energy, kinetic energy, and the zonal and eddy components of each for the period December 21, 1958–January 13, 1959. All quantities computed once daily at 0000 GMT.
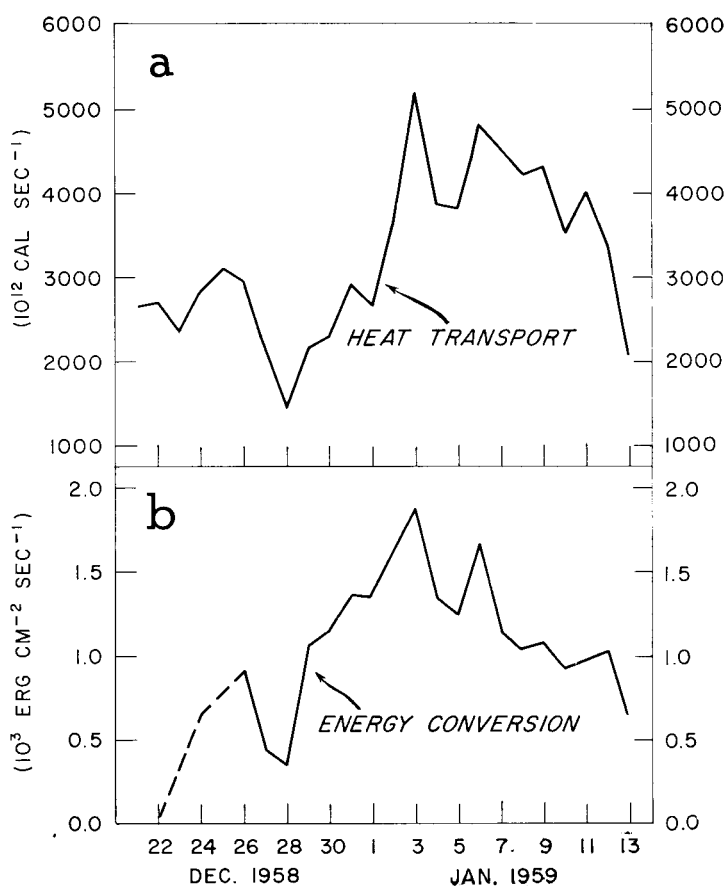

FIGURE 3.—(a) Total heat transport across all latitudes from 20° N. northward, and (b) the conversion between available potential and kinetic energy (positive for conversion to kinetic energy), for the period December 21, 1958–January 13, 1959. Both quantities computed once daily at 0000 GMT. Portion of energy conversion curve prior to December 26 is dashed since conversion data were unavailable for December 23 and 25.

constant, low level until December 29 and then began a general rise culminating in a peak value on January 4, when the zonal available potential energy was falling precipitously. Following this maximum the eddy available energy dropped at a rapid rate to reach a minimum on January 7, but a rapid rebound brought it to values only slightly less than peak values between January 8 and 12, when the zonal component reached its minimum value.

This overall behavior of the eddy relative to the zonal component of the available potential energy suggests very strongly that the increased level of eddy available energy was derived from the zonal available energy. In other words, strong thermal gradients developed *within* latitude circles at the expense of the thermal gradients *between*

latitude circles. This is supported by the variation of the total northward heat transport (summed over all latitude circles) which is shown in figure 3. Note that heat transport was at a relatively low level during the buildup of zonal available potential energy, but spurted rapidly upward at the time when the zonal available energy began to decline after January 1. In view of the direct role that heat transport plays in the conversion from zonal to eddy available potential energy (equation (12)) there is little doubt that this increase in heat transport after January 1 signified a marked increase in this energy conversion.

Turning to the kinetic energy variations in figure 2, it is seen that the total kinetic energy also went through a cycle at this time, but it was almost completely dominated by the variations in the eddy kinetic energy. Note that the eddy (and total) kinetic energy generally increased for more than a week before reaching a maximum between about January 6 and 7, more than 2 days later than the peak in the eddy available potential energy. Thus the next step in the energy flow, the transformation from

eddy available to eddy kinetic energy (see fig. 1) evidently occurred.

As for the final step in the typical energy flow, the conversion from eddy kinetic to zonal kinetic energy, there appears to be very little evidence that any appreciable increase in conversion to zonal kinetic energy was realized in this period since the zonal kinetic energy showed rather small time variations. There was, however, a weak maximum in the zonal kinetic energy on January 6, about the same time as the maximum in the eddy kinetic energy.

The conversion between total available potential and total kinetic energy shown in figure 3 generally verifies the increased flow of energy from available potential to kinetic during the first several days of January. Comparison of this conversion with the time changes in total kinetic energy that can be deduced from figure 2 shows that they were generally related in the direction indicated by equation (8); i.e., the conversion term tended to be larger when kinetic energy was markedly increasing and smaller when kinetic energy was markedly decreasing (on the assumption that D always acts to decrease kinetic energy and that it does not vary nearly so much as the conversion term).

It is interesting that the time variation of the conversion term, which is a function of the spatial covariance between vertical motion and temperature, appears to be rather well correlated with the variations in total heat transport, which is a function of the spatial covariance between meridional motion and temperature. This tends to verify the deductions of Kuo [2] that northward heat transport (and hence conversion from zonal to eddy available potential energy) and conversions from potential to kinetic energy must be closely related. However, despite this good correspondence in these quantities, the actual curves of eddy available and eddy kinetic energy (fig. 2) are imperfectly correlated, particularly near the time of maximum values in the two eddy components (January 3–9). In fact, a secondary minimum in eddy available potential energy occurred on January 7, very close to the maximum in eddy kinetic energy. The explanation for this lack of agreement probably lies in the behavior of the generation of eddy available potential energy which apparently was responsible for the downturn in eddy available energy between January 3 and 7. Some evidence for this will be presented in the following sections.

4. THE GENERATION OF AVAILABLE POTENTIAL ENERGY

It was indicated earlier that for a closed region the available potential energy can change due to either a conversion term, depending on a correlation between vertical motion and temperature, or a generation term, depending on a correlation between diabatic heating and temperature (equations (7), (9), (10)). The variations of the conversion term have already been shown (fig. 3) and discussed above. Although readily computed through
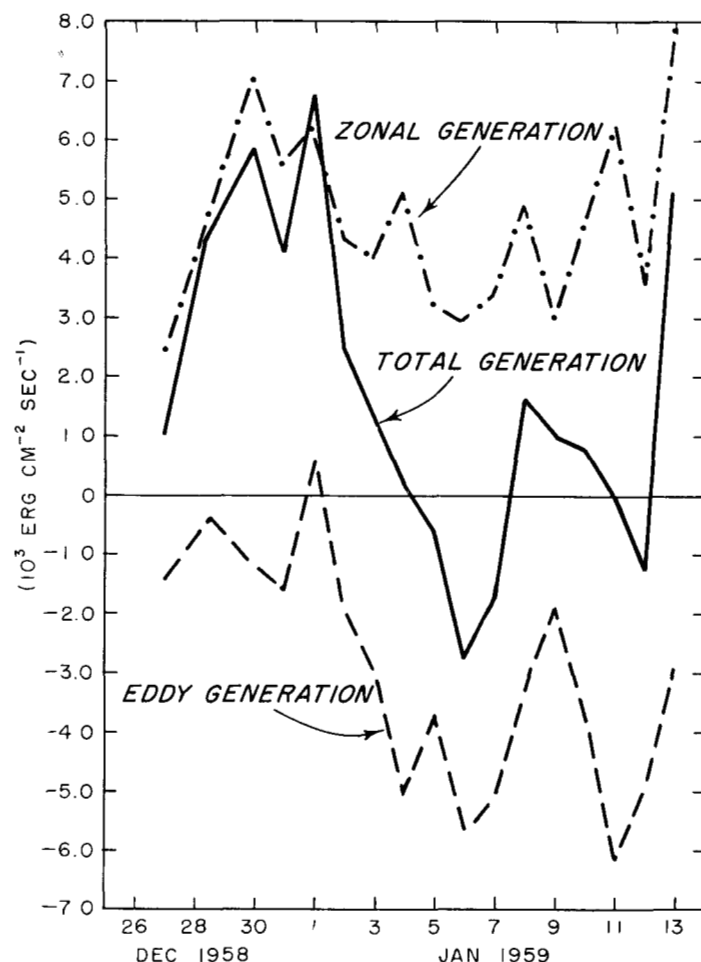

FIGURE 4.—Generation of available potential energy and its zonal and eddy components for the period December 27, 1958–January 13, 1959. Quantities computed once daily at 0000 GMT.

use of numerically calculated vertical motions its accuracy is not readily determinable. The problem of obtaining the diabatic heating, and consequently reliable estimates of the generation term however, is an even more difficult problem. Recently however, Wiin-Nielsen and Brown [15] have devised a method for computing the diabatic heating hemispherically on a daily basis. Their method essentially utilizes an equation derived from the thermodynamic energy equation where the vertical motion is estimated from the vorticity equation.

By utilizing their method it is now possible to estimate the generation of available potential energy from synoptic data, and indeed this was also done by Wiin-Nielsen and Brown. Their computations of the average generation term for the month of January 1959 indicate a value of about 1.5×10^3 ergs cm.$^{-2}$ sec.$^{-1}$, a value comparable to the average conversion from potential to kinetic energy for the same month (Wiin-Nielsen [14]). This represents the sum of 5.0×10^3 ergs cm.$^{-2}$ sec.$^{-1}$ for the zonal component and -3.5×10^3 ergs cm.$^{-2}$ sec.$^{-1}$ for the eddy component. Thus according to these calculations, the only source of available potential energy, at least during
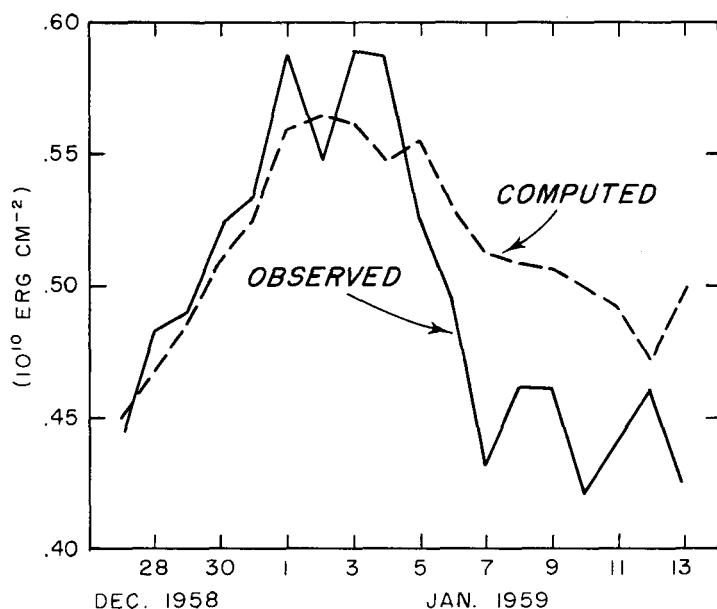
Figure 5.—Observed and computed available potential energy for the period December 27, 1958–January 13, 1959.

January 1959, was the latitudinal heating gradient. Apparently the heating within latitude circles, which represents the heating associated with the long planetary waves and transient disturbances, served only to reduce the available potential energy.

As part of the study of the cycle in available potential energy treated in this report, it was felt to be of interest to compare the interdiurnal variation of the generation term and its zonal and eddy components with that of the available potential energy. For this purpose Wiin-Nielsen has kindly made his computations for January 1959 available to us and these have been combined with similar computations made in the Meteorological Satellite Laboratory for the period December 27–31, 1958.

The time variations of these energy generation terms are shown in figure 4. As can be seen, the zonal generation was always positive, seldom dropping below 3 units, while the eddy generation was predominantly negative, averaging frequently below −2 units. The total generation, while usually positive, was occasionally negative, particularly between January 4 and 7, indicating that the heating field even in winter can at times act to destroy available potential energy. Of particular interest for this study was the similar behavior of the generation term and the total available potential energy (fig. 2) between December 27 and January 7. Both curves increased very markedly at the beginning of the period with the generation term reaching a maximum of 7×10^3 ergs cm.$^{-2}$ sec.$^{-1}$ about two days prior to the maximum in the available potential energy. At this time the eddy generation was small so that the total was nearly equal to the zonal component, reflecting a predominantly latitudinal heating distribution. Also significant is the fact that the generation term remained above 2 units for
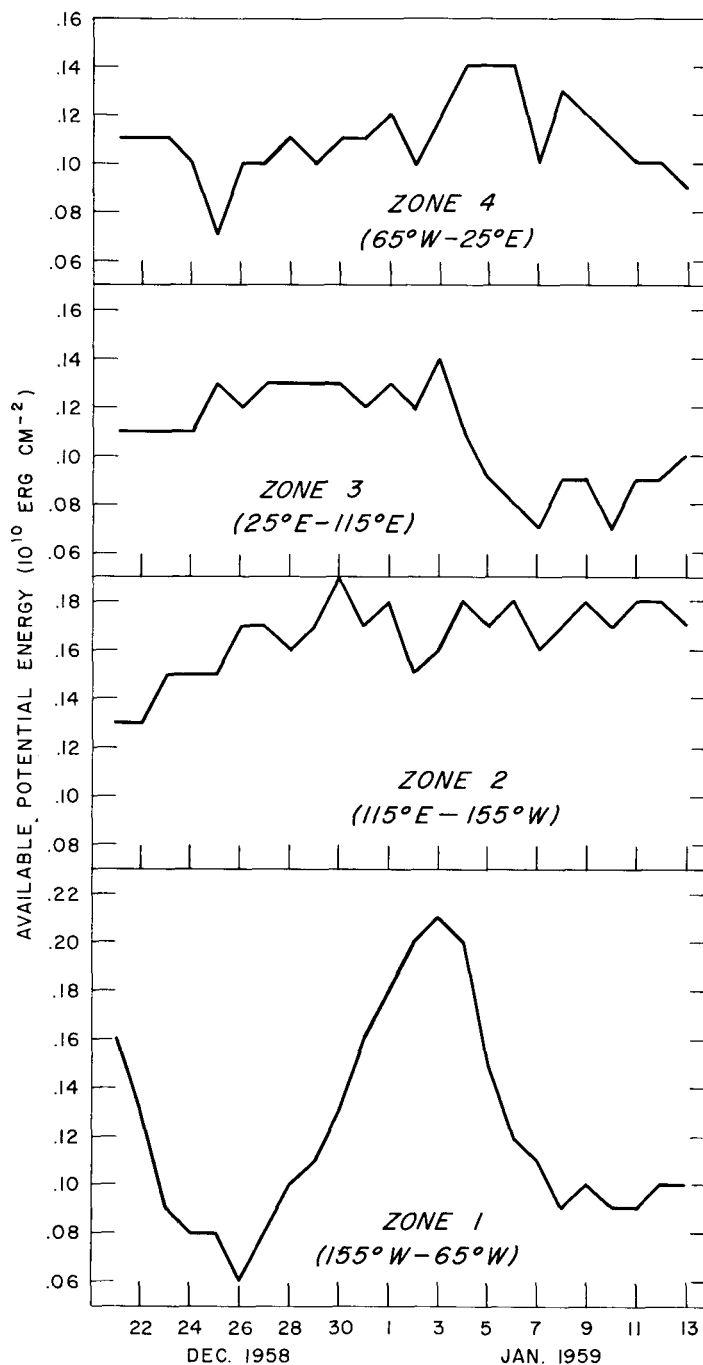

Figure 6.—Available potential energy in four zones extending northward from 30° N. within the indicated longitudinal boundaries for the period December 21, 1958–January 13, 1959. Quantities computed once daily at 0000 GMT.

about six consecutive days. Considering the magnitude of the energy conversion term (fig. 3) this was sufficient to cause an increase in available potential energy during this period.

After January 1 the intensity of the total generation of available potential energy was drastically reduced and within a few days it had even become negative. Much of this decline was due to the sudden drop in the eddy gen-
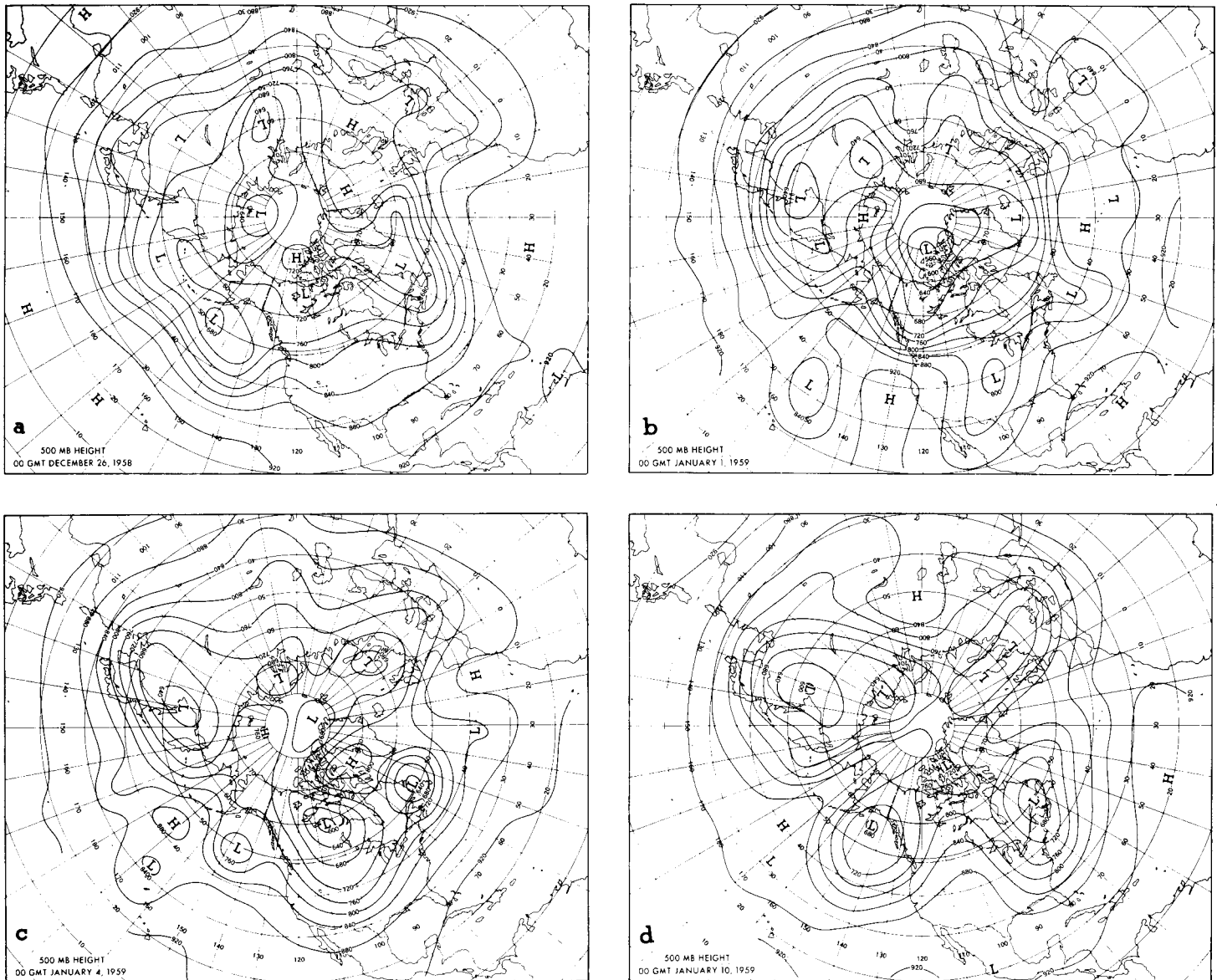
Figure 7.—500-mb. contour patterns for (a) December 26, 1958, (b) January 1, 1959, (c) January 4, 1959, and (d) January 10, 1959. Contour interval is 400 ft.

eration term which fell nearly 6 units during the same interval. This was the result of more intense cold air outbreaks and the consequent heating of polar air masses in middle and lower latitudes, as will be illustrated in the next section. The sudden dip in the eddy available potential energy between January 4 and 7 (fig. 2), which was discussed earlier, was probably a response to this strong heating and a direct consequence of the large negative value of the eddy generation. This was a period during which the computed values of both the (total) generation and (total) conversion terms contributed toward a decline in total available potential energy, agreeing with the observed decline. It is of interest in this regard to compare in more detail the computed behavior of the sum of C, the conversion term, and G the generation term, with the

observed variation in available potential energy during this period. This will now be considered.

Equation (7) may be integrated to give

$$\bar{A}_n = \bar{A}_{n-1} + (G - C)\delta t, \qquad (14)$$

where $\bar{A}_n$ is the value of available potential energy on a given day n, $\bar{A}_{n-1}$ is the value a day earlier, and δt is an interval of 1 day. Specifying the value of $\bar{A}_0$, which has been chosen here to be the observed value of the available potential energy on December 26, one can compute $\bar{A}_1$ and all succeeding values of $\bar{A}_n$ for as many days as one pleases, providing values of $G - C$ are available. These computed values of available potential energy are shown in comparison with the observed values for our period of
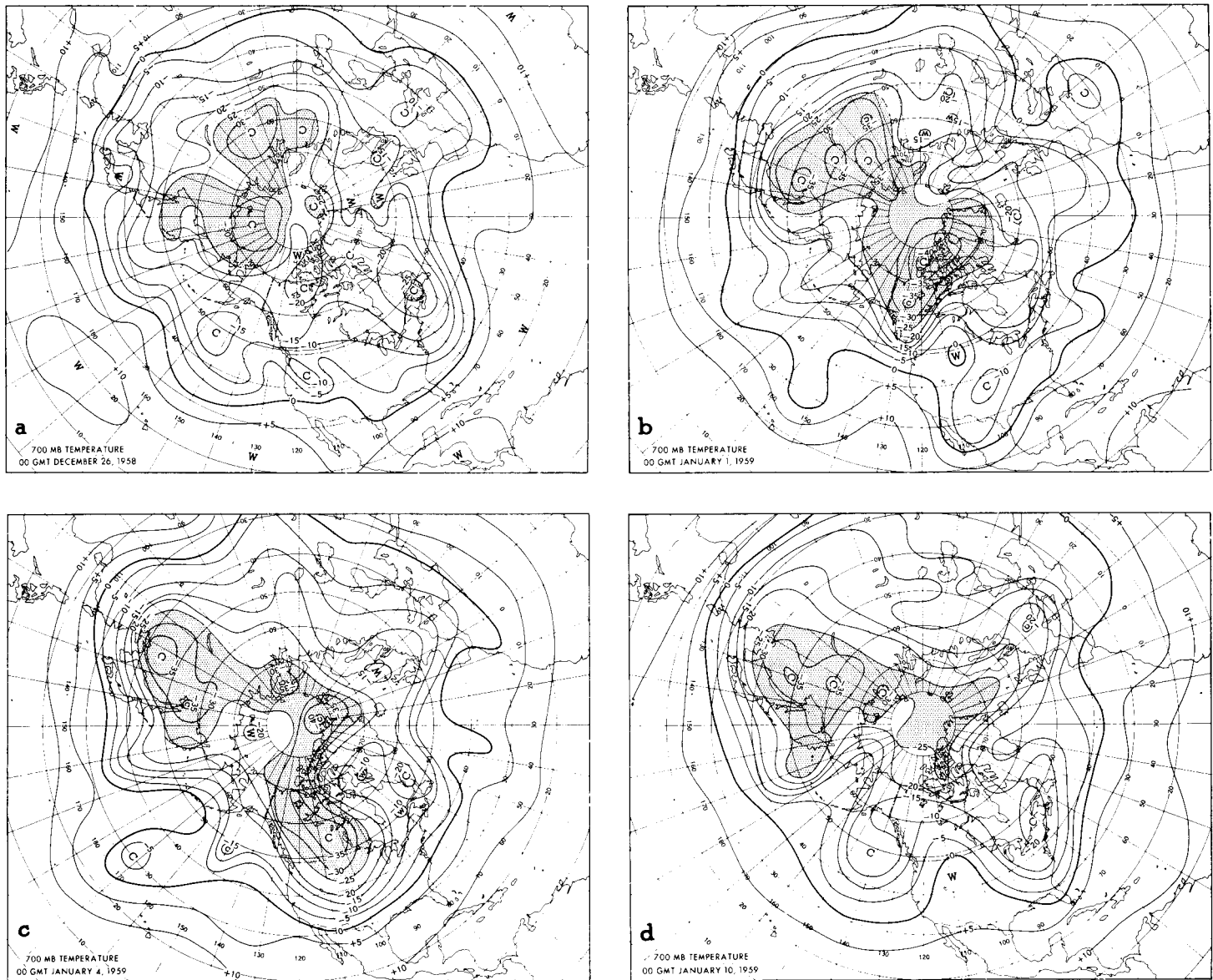
FIGURE 8.—700-mb. isotherms for (a) December 26, 1958, (b) January 1, 1959, (c) January 4, 1959, and (d) January 10, 1959. Interval is 5° C. with area below −25° C. stippled.

interest in figure 5. It is quite clear that the increase in available potential energy between December 27 and January 1 is explained very well by the sum of the generation and conversion terms, although the computed values do not rise to as high a maximum as the observed. The most serious discrepancy between computed and observed values occurred after January 3 during the period of strong decline in available potential energy. This period was represented by only a weak decline in the computed values, which suggests that the computed conversion term particularly after January 1, while indicating the correct trend, was too small. This is most likely attributable to the fact that the vertical velocities used in computing C are too small. Similar conclusions were were reached by Palmén [7], who suggested that the energy

conversion computed by this method should be increased by about 40 percent or more. The weak values of the energy conversion probably also reflect the lack of inclusion of moist adiabatic processes in the vertical motion computations. Smagorinsky [11] has indicated that when these are included the upward motions are found to be much larger than those obtained by assuming dry adiabatic motions. Since moist adiabatic effects would be expected to be larger in warm air masses, the conversion from potential to kinetic energy would also be expected to be larger.

Despite these discrepancies, the encouraging fact is that such realistic estimates of the variations in available potential energy were obtained from the generation and conversion terms, particularly since these terms were com-

puted on the basis of rather restrictive and incomplete models of the atmosphere.

5. REGIONAL AND SYNOPTIC FEATURES OF THE ENERGY CYCLE

The variations of total available potential energy shown in figure 2 were also examined from another point of view (as contrasted with the zonal and eddy components previously considered). The available potential energy was partitioned into four regional components representative of sectors 90° of longitude wide, stretching from the pole to 30° N. These four sectors were chosen somewhat arbitrarily, but roughly in such a fashion as to cover the two oceans and two continents. The longitudinal boundaries of each zone and the portion of the available potential energy contributed by each of these zones are shown in figure 6. The most striking feature of the variations of these regional components was that the major cycle of buildup and decline in available potential energy showed up only in the component of energy in Zone 1 (North America and vicinity). Thus the variations in the available potential energy for the whole Northern Hemisphere were basically dependent on the events in only this one particular region. The dominance of one area over another is not too unusual, of course, since differences in the types of flow patterns over various parts of the Northern Hemisphere have frequently been noted (cf., Namias [6]). However the virtually complete absence of an energy cycle at this time in three of the four zones is quite surprising, particularly since the total energy over all longitudes showed such a large variation.

Further insight into this energy cycle is attained through inspection of synoptic charts, which showed some interesting developments over North America and also over other portions of the hemisphere during this period. To illustrate these events, 500-mb. height and 700-mb. temperature fields for four selected days are presented in figures 7 and 8.

Confining our attention at first mainly to the North American area, we see that on December 26, when available potential energy was at a relatively low value, both over North America (Zone 1 in fig. 6) and over the hemisphere as a whole (fig. 2), there was a rather ill-defined circulation pattern (fig. 7a) with weak thermal gradients (fig. 8a). The high values of available potential energy which prevailed by January 1 were characterized by a deep cyclonic vortex over the Canadian Arctic (fig. 7b) with an associated extensive pool of cold air (fig. 8b). By January 4 a cyclonic vortex was located in western Canada, some 20° latitude south of the one in figure 7b, and the broad cyclonic flow to its south dominated most of the United States (fig. 7c). Accompanying these circulation developments, an extensive tongue of cold air covered western Canada and was also invading the United States (fig. 8c). This date marked the beginning of the overall drop in available potential energy over North America (fig. 6) and also the time of the

maximum in eddy available potential energy for the hemisphere and of a very rapid drop in the zonal available energy (fig. 2). Thus the southward penetration of cold air over North America was one of the major instrumentalities in the breakdown of the strong supply of available potential energy that had built up over North America and the hemisphere as a whole. Undoubtedly a major part of its contribution to the energy breakdown was in its role in the conversion of zonal available into eddy potential energy and thence into eddy kinetic energy, all of which occurred at this time (fig. 3).

By the final day in this sequence, January 10, when available potential energy over North America (fig. 6) and the zonal available energy for the hemisphere (fig. 2) had dropped to relatively low values again, this cyclonic vortex was located near the Gulf of St. Lawrence with its main trough extending down the east coast of the United States (fig. 7d). The cold air associated with this system was now definitely weaker than before; in fact, most of the colder air (e.g., temperatures below −25° C.) over North America had disappeared (fig. 8d). This warming was undoubtedly reflective of two processes, one the descent of the cold air which contributed to conversion from potential to kinetic energy and the other the heating of the cold air mass as it proceeded off the east coast out over the Atlantic. Very large amounts of heating were computed by Wiin-Nielsen and Brown [15] on the days when the cold air moved off the coast (January 5–6) and it is evident that the strong heating of this cold air contributed to the strong negative values of computed eddy generation on these days (fig. 4).

Turning to other features of the flow and thermal fields it is of interest to note that a considerable amount of cold air was present over eastern Asia on each of the days shown in figure 8. This was very likely associated with the relatively high level of available potential energy in Zone 2 between December 26 and January 10 (fig. 6). Also, while a portion of this cold air was located farther west in Siberia (figs. 8a, 8b), the level of available energy in Zone 3 was fairly high, but as most of it moved east of Lake Baikal (figs. 8c, 8d) a noticeable drop in the energy in Zone 3 occurred. This more narrow longitudinal organization of the cold air near the Asian coast was accompanied by the sharpening of the Asian coastal trough subsequent to January 1 (fig. 7). Although the total energy for Zone 2 remained virtually the same, computations of longitudinal contributions to the northward heat transport (Winston [16]) showed that substantial heat transports were effected by the Asian coastal trough subsequent to January 1. This signified that increased transformations from zonal to eddy available energy occurred in this zone during the period of development of increased eddy energy in January (fig. 2). Thus, despite the lack of a cycle in the overall energy, it appears that eddy Zone 2 (eastern Asia to the east central Pacific) did contribute toward the increase or maintenance of eddy energy.
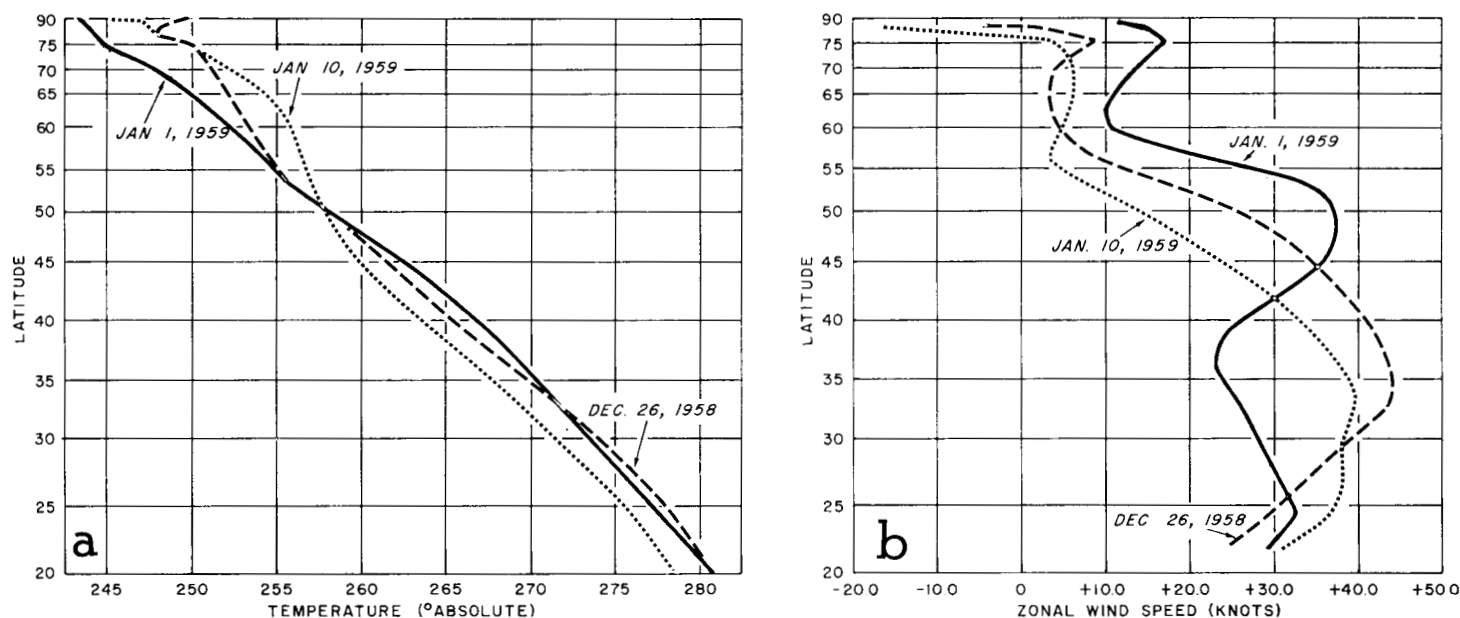
FIGURE 9.—Latitudinal profile of (a) temperature and (b) zonal wind speed for December 26, 1958 (dashed), January 1, 1959 (solid), and January 10, 1959 (dotted).

Finally it is worth noting that the overall hemispheric flow pattern at the end of the energy cycle (January 10, fig. 7d) consisted of four major, large-amplitude waves with large cyclone centers in middle latitudes. As indicated in figure 2, this was a day of minimum zonal available potential energy, but with fairly large eddy available potential energy. This pattern is to be contrasted with (1) the more heterogeneous (although mainly zonal) flow pattern of December 26 (fig. 7a), before zonal available energy started increasing; (2) the zonal flow at higher latitudes surmounting large-amplitude waves at lower latitudes of January 1 (fig. 7b), when zonal available energy was at its peak and eddy available energy was building up; and (3) the pattern of increasing wave amplitudes on January 4 (fig. 7c) when zonal available energy was dropping rapidly and eddy available energy was at a peak.

The latitudinal profiles of zonal wind and temperature for the whole hemisphere for three of these days summarize some of the differences at these different stages further (fig. 9). Note that at the beginning (December 26) and end (January 10) of the cycle there were rather broad zones of westerlies with maximum speeds located near latitude 35°. The flow at the end of the cycle was generally weaker than at the beginning except south of 30°. By way of contrast the westerlies on January 1 were concentrated in a narrow zone in middle latitudes (peak near 50°) with a definite minimum in the flow near 35° and a secondary maximum near 25°. These profiles are roughly characteristic of the zonal wind distributions at various phases of the index cycle (cf., Namias [5]), but it is worth pointing out that the profile for January 1

does not represent a case of extremely high zonal index (in latitudes 35°–55° N.).

The thermal profiles show rather definitely that the peak zonal available energy (January 1) was marked by rather low temperatures north of 55°, a cooling of up to 5° C. from December 26. This high-latitude cooling during a period when the westerlies were strengthening near latitudes 45°–55° was essentially the same type of development which Namias [5] described as containment of cold air in the polar cap during periods of strong westerly flow. By January 10, when the zonal available energy was at its lowest, temperatures were considerably higher north of 50°. The outflow of cold air into middle and lower latitudes in connection with the conversion of zonal available into eddy available energy is strikingly clear. Or putting it another way, the effects of the increased heat transports subsequent to January 1 were quite marked in the reduction of the northward thermal gradient.

6. SUMMARY

This observed cycle of available potential energy for the Northern Hemisphere possessed many characteristics which had been deduced from previous evaluations of some long-period averages of energy parameters and energy conversion terms. The buildup in zonal available energy to a high value and then its subsequent breakdown with the accompanying conversion into eddy available potential and eddy kinetic energy have all been clearly demonstrated. There was, however, little if any reaction to this potential energy cycle in the zonal component of the kinetic energy. The fact that estimates of energy

conversion and energy generation obtained from admittedly crude atmospheric models showed rather good correspondence with the observed short-period variations in the various energy parameters was especially interesting. The partition of available potential energy on a regional (longitudinal) basis showed that this clear-cut cycle in hemispheric available potential energy was dominated to a remarkable extent by events in only about one-quarter of the hemisphere. Investigations of the synoptic aspects of this energy cycle showed that this dominance by one region (North America and vicinity) was associated with the development of cold air over the Canadian Arctic and then the subsequent southward penetration of this large mass of cold air into the United States and out over the Atlantic. Obviously this signifies that studies of atmospheric energetics require close attention to geographical and synoptic-scale influences.

Although this cycle displayed many characteristics of the idealized energy cycle, it should not be concluded that this observed cycle is truly typical of most large-scale energy cycles. Cursory inspection of an accumulating record of available potential energy over more than a year indeed reveals that large-scale variations of the zonal and eddy components of the potential energy occur in a variety of ways. Study of the nature of other large-scale changes in the energy is contemplated, particularly with respect to probable differences in the manner in which the potential energy is generated.

ACKNOWLEDGMENTS

REFERENCES

1. C. E. Jensen, "Energy Transformation and Vertical Flux Processes Over the Northern Hemisphere," *Journal of Geophysical Research*, vol. 66, No. 4, April 1961, pp. 1145–1156.
2. H. L. Kuo, "Application of Energy Integrals to Thermally Driven Motions," *Beiträge zur Physik der Atmosphäre*, vol. 31, No. 3/4, 1959, pp. 189–199.
3. E. N. Lorenz, "The Basis for a Theory of the General Circulation," Section IV of "Studies of the Atmospheric General Circulation," ed. by V. P. Starr, *Final Report* Part I, General Circulation Project, Contract AF 19(122)–153, Department of Meteorology, Massachusetts Institute of Technology, May 1954, pp. 522–534.
4. E. N. Lorenz, "Available Potential Energy and the Maintenance of the General Circulation," *Tellus*, vol. 7, No. 2, May 1955, pp. 157–167.
5. J. Namias, "The Index Cycle and Its Role in the General Circulation," *Journal of Meteorology*, vol. 7, No. 2, Apr. 1950, pp. 130–139.
6. J. Namias, "Thirty-Day Forecasting: A Review of a Ten Year Experiment," *Meteorological Monographs*, vol. 2, No. 6, American Meteorological Society, Boston, 1953, 83 pp.
7. E. Palmén, "On Generation and Frictional Dissipation of Kinetic Energy in the Atmosphere," *Societas Scientiarum Fennica, Commentationes Physico-Mathematicae* vol. XXIV, No. 11, 1960, 15 pp.
8. N. A. Phillips, "The General Circulation of the Atmosphere: A Numerical Experiment," *Quarterly Journal of the Royal Meteorological Society*, vol. 82, No. 352, Apr. 1956, pp. 123–164.
9. C. G. Rossby and H. C. Willett, "The Circulation of the Upper Troposphere and Lower Stratosphere, "*Science*, vol. 108, Dec. 10, 1948, pp. 643–652.
10. B. Saltzman and A. Fleisher, "The Modes of Release of Available Potential Energy in the Atmosphere," *Journal of Geophysical Research*, vol. 65, No. 4, Apr. 1960, pp. 1215–1222.
11. J. Smagorinsky, "On the Inclusion of Moist Adiabatic Processes in Numerical Prediction Models," In *Symposium über Numerische Wettervorhersage in Frankfort a.M. vom 23. bis 28. Mai 1956. Berichte des Deutschen Wetterdienstes*, Nr. 38, (Band 5), 1956.
12. J. Smagorinsky, "General Circulation Experiments with the Primitive Equations as a Function of the Parameters," (To be published) Abstract in *Programme of Meetings, International Association of Meteorology and Atmospheric Physics*, XII General Assembly, I.U.G.G., Helsinki, July 26–Aug. 6, 1960. pp. 22–23.
13. R. M. White and B. Saltzman, "On Conversions Between Potential and Kinetic Energy in the Atmosphere," *Tellus*, vol. 8, No. 3, Aug. 1956, pp. 357–363.
14. A. Wiin-Nielsen, "A Study of Energy Conversion and Meridional Circulation for the Large-Scale Motion in the Atmosphere," *Monthly Weather Review*, vol. 87, No. 9, Sept. 1959, pp. 319–332.
15. A. Wiin-Nielsen and J. A. Brown, Jr., "On the Distribution of Heat Sources and Sinks in the Lower Troposphere and the Corresponding Generation of Potential Energy," (To be published in the *Proceedings of the International Symposium on Numerical Weather Prediction, Tokyo, Japan, Nov. 7–13, 1960.*)
16. J. S. Winston, "Preliminary Studies of Atmospheric Energy Parameters," *Meteorological Satellite Laboratory Report to the National Aeronautics and Space Administration, No. 3*, U.S. Weather Bureau, January 1961, 30 pp.